



# Investigation of phenyllactic acid as a potent tyrosinase inhibitor produced by probiotics

Minhye Shin<sup>a,b,1</sup>, Van-Long Truong<sup>c,1</sup>, Minjee Lee<sup>d</sup>, Donggyu Kim<sup>a,b</sup>, Myun Soo Kim<sup>e</sup>, Hana Cho<sup>e</sup>, Young Hoon Jung<sup>c</sup>, Jungwoo Yang<sup>d,\*</sup>, Woo Sik Jeong<sup>c,\*\*</sup>, Younghoon Kim<sup>f,\*\*\*</sup>

<sup>a</sup> Department of Microbiology, College of Medicine, Inha University, Incheon, 22212, Republic of Korea

<sup>b</sup> Department of Biomedical Science, Program in Biomedical Science and Engineering, Inha University, Incheon, 22212, Republic of Korea

<sup>c</sup> Food and Bio-industry Research Institute, School of Food Science & Biotechnology, College of Agriculture and Life Sciences, Kyungpook National University, Daegu, 41566, Republic of Korea

<sup>d</sup> Ildong Bioscience, Pyeongtaek-si, Gyeonggi-do, 17957, Republic of Korea

<sup>e</sup> ICBIO, Cheonan-si, Chungcheongnam-do, 31027, Republic of Korea

<sup>f</sup> Department of Agricultural Biotechnology, Research Institute of Agriculture and Life Science, Seoul National University, Seoul, 08826, Republic of Korea

## ABSTRACT

Melanogenesis is responsible for skin pigmentation and the enzymatic browning of foods. Tyrosinases play a major role in melanin synthesis, and many attempts have been made to identify new natural tyrosinase inhibitors, but few have sought to do in microbes. Postbiotics are bioactive compounds produced by the metabolism of probiotics and have been reported to be safe and effective. In this study, we evaluated the tyrosinase inhibitory effects of culture supernatants of probiotics and discovered novel bacterial metabolites that can be used as a potent tyrosinase inhibitor based on metabolomics. Cultures of *Bifidobacterium bifidum* IDCC 4201 and *Lactiplantibacillus plantarum* IDCC 3501 showed effective anti-tyrosinase, reduced melanin synthesis, and altered protein expression associated with the melanogenesis pathway. Comparative metabolomics analyses conducted by GC-MS identified metabolites commonly produced by *B. bifidum* and *L. plantarum*. Of eight selected metabolites, phenyllactic acid exhibited significant tyrosinase-inhibitory activity. Our findings suggest that applications of probiotic culture supernatants containing high amounts of phenyllactic acid have potential use as anti-melanogenesis agents in food and medicines.

## 1. Introduction

Melanogenesis is a multistage biochemical process of melanin biosynthesis that involves the oxidation and subsequent polymerization of tyrosine in melanocytes. Skin pigmentation is an important phenotypic trait that plays a critical role in photoprotection by absorbing ultraviolet radiation and thus preventing skin damage from sun exposure and skin photocarcinogenesis (Brenner and Hearing, 2008). Defective melanogenesis can result in hypo or hyperpigmentation, which negatively impact quality of life and cosmesis. Therefore, the food and cosmetic industries have invested heavily in means of regulating skin pigmentation (Ebanks et al., 2009).

Of the enzymatic reactions involved in melanin biosynthesis, tyrosinases (multifunctional copper-containing metalloenzymes) play central roles as rate-limiting enzymes (Zolghadri et al., 2019). Tyrosinases catalyze the oxidation of L-tyrosine to DOPA-quinone using bifunctional

monophenolase-diphenolase activities via the production of L-3, 4-dihydroxyphenylalanine (L-DOPA) (referred to as the Raper Mason pathway), which results in the synthesis of eumelanin (Mason, 1948; Raper, 1928).

Tyrosinase inhibitors produced by plants, fungi, and bacteria are viewed as attractive potential skin-whitening agents due to their low toxicities and bioavailabilities, especially for food and cosmetic applications (El-Nashar et al., 2021), and the tyrosinase inhibitory activities of many indigenous plant extracts have been reported in Korea, Brazil, Japan, and Bangladesh (Hun Son and Young Heo, 2013; Souza et al., 2012). However, although several tyrosinase inhibitors have been identified in plants, including phenolics, steroids, and alkaloids, relatively little research has been undertaken on candidate inhibitors of microbial origin. Thus, only a small number of bacterial metabolites, e. g., alkaloids and macrolides, that inhibit tyrosinase have been identified (Ishihara et al., 1991).

\* Corresponding author.

\*\* Corresponding author.

\*\*\* Corresponding author.

E-mail addresses: [yjw@ildong.com](mailto:yjw@ildong.com) (J. Yang), [wsjeong@knu.ac.kr](mailto:wsjeong@knu.ac.kr) (W.S. Jeong), [ykeys2584@snu.ac.kr](mailto:ykeys2584@snu.ac.kr) (Y. Kim).

<sup>1</sup> These authors contributed equally to this work.

Probiotics are live bacteria that benefit the host by producing useful physiologically bioactive compounds. These compounds have been reported to have immunomodulatory, anti-carcinogenic, anti-aging, and anti-microbial effects, but their utilities are currently limited by a lack of knowledge of their molecular mechanisms, strain-specific behaviors, and safeties (Bourehaba et al., 2022; Rodríguez-Pastén et al., 2022). To address these limitations, studies have recently focused on postbiotic molecules, which are defined as metabolic products secreted by probiotics in cell-free supernatants (Nataraj et al., 2020). A number of studies have revealed various effects of postbiotic molecules on human diseases including anti-microbial, anti-inflammatory, anti-oxidative, and anti-cancer activities (Nataraj et al., 2020). These molecules involve bacteriocins, short chain fatty acids, vitamins, and phenolic compounds. Several studies reported that *Lactobacillus helveticus*, *Lactobacillus acidophilus*, and *Lactobacillus gasseri* suppressed melanin production by inhibiting tyrosinase (Ikarashi et al., 2020; S. Lee et al., 2022; Lim et al., 2020, p. 12625). However, specific postbiotic metabolites associated with anti-melanogenesis have not been identified yet. In this study, we identified specific probiotic strains that produce supernatants with promising melanogenic inhibitory activities. Using GC-MS-based metabolomics analyses, metabolites with tyrosinase inhibitory activities were identified and investigated.

## 2. Materials and methods

### 2.1. Bacterial culture

Probiotic strains used in this study were kindly gifted from Ildong Bioscience. Bacterial cultures were prepared as previously reported in (Shin et al., 2021). Specifically, probiotic strains (*Lactocaseibacillus rhamnosus* IDCC 3201, *Lactobacillus acidophilus* IDCC 3302, *Lactocaseibacillus paracasei* IDCC 3401, *Lactiplantibacillus plantarum* IDCC 3501, *Bifidobacterium bifidum* IDCC 4201, and *Bifidobacterium breve* IDCC 4401) were anaerobically cultured at a cell density at  $10^9$  CFU/mL in De Man, Rogosa and Sharpe medium (MRS; BD Difco, Franklin Lakes, NJ, USA) for 18 h at 37 °C. Cells were collected by centrifugation at 2600 rpm for 10 min and filtered through a 0.22 µm syringe filter.

### 2.2. Tyrosinase inhibition assay

Tyrosinase inhibition assays were performed using L-tyrosine (Sigma, St. Louis, MO, USA) and L-DOPA (Sigma) as substrates for monophenolase and diphenolase, respectively, as previously reported (Noh et al., 2020) with slight modifications. The reaction mixture (140 µL) contained 110 µL of phosphate buffer (0.1 M, pH 6.5), 1 µL of mushroom tyrosinase ( $25,000 \text{ U mL}^{-1}$ , Sigma) and 20 µL of 5 mM L-tyrosine or L-DOPA with probiotic culture supernatant (final 10 and 20%, v/v). Reaction mixtures were monitored at 475 and 490 nm for dopachrome formation. All measurements were made in triplicate. To assay the tyrosinase inhibitory effects of individual metabolic compounds, candidate inhibitors (alanine, leucine, methionine, phenylalanine, threonine, valine, pipecolic acid, or phenyllactic acid; Sigma) were added to reaction mixtures at concentrations of 10 or 20 mM. Tyrosinase activities (%) were calculated by expressing supernatant absorbance as a percentage of the absorbance of vehicle controls.

### 2.3. Melanocytes culture and quantification of melanin contents

Murine melanoma cell line B16F10 was purchased from the Type Culture Collection and cultured in Dulbecco's modified Eagle's medium (Gibco, Waltham, MA, USA) supplemented with 10% fetal bovine serum (FBS) and 1% penicillin/streptomycin at 37 °C in a humidified 5% CO<sub>2</sub> incubator. Murine melan-a cell line, an immortal line of pigmented melanocyte, was kindly gifted from Prof. Nam-Joo Kang (Kyungpook University, Daegu, Republic of Korea) and maintained in Roswell Park Memorial Institute 1640 medium (Gibco, Waltham, MA, USA)

supplemented with 10% FBS and 1% penicillin/streptomycin at 37 °C in a humidified atmosphere with 5% CO<sub>2</sub>.

For melanin quantification, the cells were treated with alpha-melanocyte-stimulating hormone ( $\alpha$ -MSH, 200 nM; Sigma) in the presence or absence of 2% probiotic culture supernatants of *L. rhamnosus*, *L. plantarum*, or *B. bifidum* for 3 days. Arbutin (100 µg/mL; Sigma) was used as a positive control (Jin et al., 2012). Through the extensive screening studies on the parameters for melanin quantification including several absorbance wavelengths (405, 475, and 490 nm), measurement of melanin absorbance at 405 nm was selected. After treatment, treated cells were collected and cell pellets were dissolved in 1 N NaOH containing 80% DMSO at 80 °C for 1 h, and melanin contents were estimated at 405 nm using a microplate reader (BioTek, Winooski, VT, USA). To assess the extra cellular level of melanin, 200 µL of cell culture media was transferred to a 96-well plate and the absorbance was measured at 405 nm using a microplate reader (BioTek).

### 2.4. Western blotting

Treated cells were homogenized in RIPA buffer (Cell Signaling Technology, Beverly, MA, USA) for 1 h on ice. Protein concentration was measured using a BCA protein assay kit (Pierce Biotechnology, Waltham, MA, USA). Equal amounts of proteins were separated on SDS-PAGE gels and then transferred to Immobilon-P membranes (Millipore, Billerica, MA, USA) using a semi-dry transfer system (Bio-Rad, Hercules, CA, USA). After blocking with 5% non-fat milk for 2 h in room temperature, the membranes were hybridized with specific primary antibodies at 4 °C overnight and subsequently incubated with proper horseradish peroxidase-conjugated secondary antibodies at 4 °C for 3 h. Finally, protein bands were visualized using a Western blotting luminol reagent (Santa Cruz Biotechnology, Santa Cruz, CA, USA).

### 2.5. Metabolite profiling

Metabolite profiling was performed as previously reported in (Park et al., 2018). Probiotic culture supernatant (750 µL) were diluted in 2.25 mL of ice-cold methanol and vortexed for 1 min, followed by centrifugation at 13,000 g for 10 min at 4 °C (Labogene, Seoul, Korea). One-hundred microliter of supernatants were collected, concentrated to dryness in a vacuum concentrator, and stored at −80 °C until required. Samples were derivatized by adding 30 µL of a solution of 20 mg/mL methoxyamine hydrochloride in pyridine (Sigma) for 90 min at 30 °C, and then adding 50 µL of N, O-bis(trimethylsilyl)trifluoroacetamide (BSTFA; Sigma) and heating for 30 min at 60 °C. A mixture of alkane standards (Sigma) and fluoranthene (Sigma) was used as retention indices and an internal standard, respectively. GC-MS analysis was conducted using a Thermo Trace 1310 GC (Thermo, Waltham, MA, USA) coupled to a Thermo ISQ LT single quadrupole mass spectrometer (Thermo). GC was performed using a DB-5MS column (60-m length, 0.25 mm i.d., and 0.25-µm film thickness) (Agilent, Santa Clara, CA, USA). Derivatized samples were injected at 300 °C using a split ratio of 1:5, and metabolites were separated using a helium flow of 1.5 mL using the following oven program; 2 min at 50 °C, 50 °C–180 °C at 5 °C/min, 8 min at 180 °C, 180 °C–210 °C at 2.5 °C/min, 210 °C–325 °C at 5 °C/min, and 10 min at 325 °C. Mass spectra were acquired in the scan range 35–650 m/z at 5 spectra per sec in electron impact ionization mode and an ion source temperature of 270 °C. Spectra were processed using Thermo Xcalibur software (Thermo) with automated peak detection, and metabolites were identified by matching mass spectra and retention indices using the NIST Mass spectral search program (version 2.0, Gaithersburg, MD, USA). Metabolite intensities were normalized with respect to the fluoranthene internal standard.

### 2.6. Molecular docking simulation

The docking simulation was performed using AutoDock Vina, an

open-source tool for molecular docking and virtual screening (Trott and Olson, 2010). Simulation results were visualized using UCSF Chimera ViewDock extension, and energy scores were compared for each ligand using the Vina algorithm (Trott and Olson, 2010).

## 2.7. Statistical analysis

For univariate analysis, one-way ANOVA and Student's t-test were conducted using GraphPad Prism 8 (San Diego, CA, USA). For metabolomics analysis, resulting data sets were analyzed by multivariate analysis using Prism and ClustVis (<https://biit.cs.ut.ee/clustvis>) used for visualizing the clustering of multivariate data (Metsalu and Vilo, 2015). Metabolites were mapped into a molecular network using the ChemViz application in Cytoscape (<http://www.rbvi.ucsf.edu/cytoscape/chemViz2/index.html>). Nodes represent structurally identified metabolites indicated by different colors.

## 3. Results and discussion

### 3.1. Screening of probiotic culture supernatants for tyrosinase inhibition

Probiotics have been reported to help prevent and treat skin diseases, such as pigmentary disorders and melanoma, and to suppress enzymatic browning of fruits and vegetables by inhibiting tyrosinase (Tsai et al., 2021; Yu et al., 2020). Tyrosinase is a multifunctional oxidase that catalyzes the hydroxylation of monophenols, such as tyrosine, to o-diphenols (DOPA) and subsequently oxidizes o-diphenols to o-quinones (DOPA quinone) (Muñoz-Muñoz et al., 2010; Slominski et al., 1989). Recent studies have focused on the bioactive compounds with beneficial effects on human health produced by probiotics, but specific probiotic small molecules for tyrosinase inhibition have not been reported yet.

To identify probiotic strains with anti-tyrosinase activity, we evaluated the tyrosinase activities of the culture supernatants from seven commercial *Lactobacillus* and *Bifidobacterium* strains that are widely used as probiotic supplements (Shin et al., 2021). Most of the strains inhibited the monophenolase activity of tyrosinase, except *L. rhamnosus* (Fig. 1A). The supernatant of *L. plantarum* and *B. bifidum* inhibited tyrosinase activity compared to other strains. To test the effects of postbiotics on diphenolase activity, we analyzed the oxidation of DOPA by tyrosinase in the presence of bacterial culture supernatants (Fig. 1B). As was observed for tyrosine hydroxylation, DOPA-tyrosinase was inhibited by the supernatants of *L. plantarum* least even at 10% of concentration. Based on these screening results, *L. plantarum* and *B. bifidum* were selected as probiotic and anti-melanogenesis candidates.

### 3.2. Effects of the selected probiotic culture supernatants on melanocyte melanin contents

B16F10 and Melan-a cell lines induced with  $\alpha$ -melanocyte stimulating hormone ( $\alpha$ -MSH) were used to examine the effects of culture supernatants on melanin synthesis (Fig. 2). The cells were incubated in media containing 2% of probiotic culture supernatants for 3 days. Induction of B16F10 cells with  $\alpha$ -MSH increased melanin content 1.3-fold, and arbutin (a positive control) significantly inhibited the melanogenesis of these cells (Fig. 2A). Culture supernatants of *B. bifidum* significantly inhibited melanogenesis, as determined by extracellular, intracellular, and total melanin contents, to 0.6–0.8-fold as compared with  $\alpha$ -MSH induced controls, and had a greater inhibitory effect than other probiotic cultures. Furthermore, *B. bifidum* culture supernatant and arbutin had similar inhibitory effects.

In Melan-a cells, culture supernatants of *L. plantarum*, *B. bifidum*, and *L. rhamnosus* (a negative-control strain) inhibited melanin synthesis as compared with  $\alpha$ -MSH induced controls (Fig. 2B). *L. plantarum* and *B. bifidum* significantly inhibited total melanin contents to 0.7- and 0.8-fold, respectively, compared with  $\alpha$ -MSH induced controls.

*L. plantarum* inhabits various ecological niches such as plants, mammalian intestines, and fermented foods (Fidanza et al., 2021). A number of studies have reported that *L. plantarum* has beneficial effects on gastrointestinal health, for example, that it improved intestinal barrier function (Wang et al., 2018) and ameliorated the symptoms of irritable bowel syndrome (Ducrotte et al., 2012) and gastritis (Zhou et al., 2021). *B. bifidum* is frequently found in the fecal samples of breast-fed infants (Turroni et al., 2012), and is considered to have remarkable physiological features, for example, to adhere to gut epithelia and to utilize host-derived glycans in the human gut (Turroni et al., 2014). Huang et al. reported a culture filtrate of *B. bifidum* exhibited dose-dependent anti-melanogenic and anti-oxidative effects (Huang et al., 2011), and Kim et al. reported that lipoteichoic acid, a cell-wall component of Gram-positive bacteria isolated from *L. plantarum*, inhibited melanogenesis (Kim et al., 2015). These reports support our findings regarding the anti-melanogenesis effects of *L. plantarum* and *B. bifidum* culture supernatants.

### 3.3. Western blot analyses of melanocytes treated with probiotic culture supernatants

Melanin is synthesized in the melanosomes of epidermal melanocytes and then transferred to keratinocytes (Pavan and Sturm, 2019).  $\alpha$ -MSH stimulates melanin production by binding to G protein-coupled melanocortin type I receptor (MC1R) and thus activating adenylate cyclase. Activation of kinase cascades results in the upregulation of microphthalmia-associated transcription factor (MITF), a basic helix-loop-helix protein crucial for melanocyte differentiation and

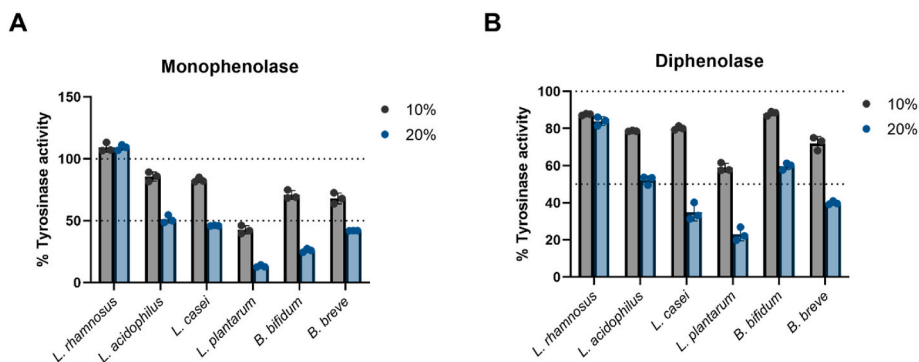


**Fig. 1.** Inhibitions of tyrosinase activity by probiotics culture supernatants. Monophenolase (A) and diphenolase (B) activities were determined using L-tyrosine and L-DOPA, respectively, as substrates. Probiotic culture supernatants were added for the final concentration of 10% and 20% (v/v) to reaction mixtures. Data are expressed as the means  $\pm$  SDs of three independent experiments.

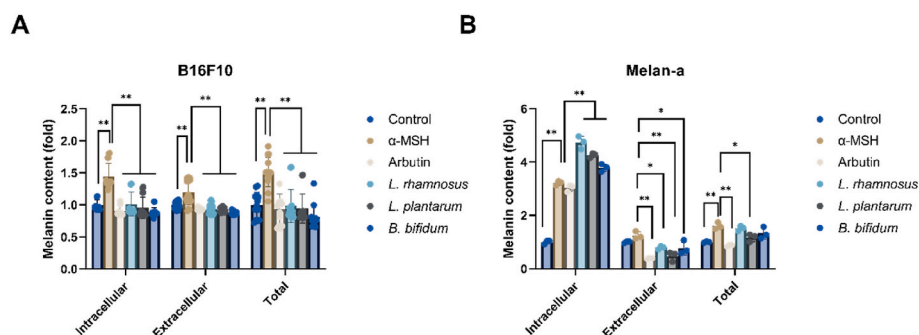


**Fig. 2.** Inhibition of melanin synthesis in skin melanocytes by probiotics culture supernatants. Melanin contents were measured in  $\alpha$ -MSH-induced B16F10 (A) and Melan-a (B) cell lines. Arbutin and *L. rhamnosus* supernatant were used as positive and negative controls for inhibiting melanin synthesis, respectively. Melanin content is represented by fold changes compared to the melanin contents in the control cells without  $\alpha$ -MSH induction. Data are expressed as the means  $\pm$  SDs of > three independent experiments. The analysis was conducted by one-way ANOVA followed by Dunnett's test for post-hoc analysis. Significant differences are indicated as \* ( $P < 0.05$ ) and \*\* ( $P < 0.01$ ).

pigmentation. Tyrosinase, a target gene of MITF, is essential for melanogenesis and with tyrosinase-related protein (TRP)-1/2 catalyzes the rate-limiting steps in the melanin synthetic pathway.

Based on our observations that probiotic culture supernatants reduced melanogenesis in melanocytes, we examined how the expressions of specific proteins (MC1R, MITF, TRP1/2 and tyrosinase) involved in melanogenesis were affected by these culture supernatants. In B16F10 cells,  $\alpha$ -MSH induction induced the expressions of MITF, TRP1/2, tyrosinase, and MC1R (Fig. 3A). When we compared protein expressions in B16F10 cells treated with probiotic culture supernatants, all three strains significantly suppressed the expressions of MITF and TRP1/2, which possibly explains why the culture supernatant of *L. rhamnosus* reduced melanin synthesis like *B. bifidum* and *L. plantarum* in B16F10 cells. The culture supernatants of *B. bifidum* and *L. plantarum* both showed significantly reduced the expressions of MITF, TRP1/2, and tyrosinase in B16F10 cells.

As was observed in B16F10 cells, probiotic culture supernatants reduced the expressions of MC1R, TRP1, and tyrosinase in Melan-a cells

(Fig. 3B). The expression of MC1R was significantly inhibited by *L. rhamnosus* and *B. bifidum* supernatants, and both had greater inhibitory effects on the expressions of TRP1 and tyrosinase than the culture supernatant of *L. rhamnosus*. The findings indicate *B. bifidum* and *L. plantarum* supernatants specifically inhibit the expression of tyrosinase in  $\alpha$ -MSH-induced melanocytes.

#### 3.4. Global metabolite profiling of selected probiotic culture supernatants

Based on the observed tyrosinase inhibitory effects of *L. plantarum* and *B. bifidum* culture supernatants, we analyzed metabolite profiles of these supernatants using *L. rhamnosus* supernatant as a negative control (Fig. 4A). A total of 80 metabolites were identified, which included amino acids, polyamines, organic acids, sugars, and free fatty acids. Principal component analysis of the identified metabolites showed a metabolic difference between the three strains (Fig. 4B;  $R^2X$ , 0.57 and  $Q^2$ , 0.71). Loading plots of the metabolome indicated specific metabolites representative for the metabolic separation (Fig. 4C).

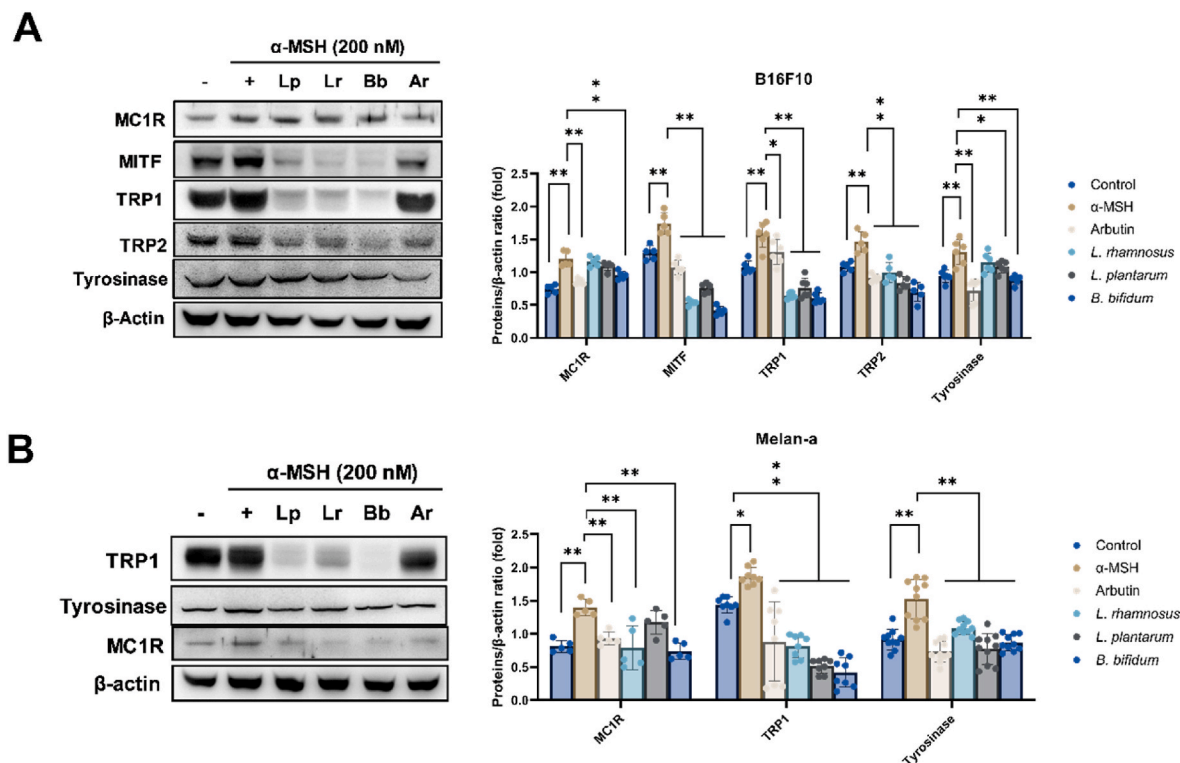


**Fig. 3.** Effects of probiotic culture supernatants on the expressions of melanogenesis-associated proteins. MC1R, MITF, TRP1, TRP2, and tyrosinase levels were determined in  $\alpha$ -MSH-induced B16F10 (A) and Melan-a (B) cells. Arbutin and *L. rhamnosus* supernatant were used as positive and negative inhibitor controls, respectively. Data are expressed as the means  $\pm$  SDs of > three independent experiments. The analysis was conducted by one-way ANOVA followed by Dunnett's test for post-hoc analysis. Significant differences are indicated as \* ( $P < 0.05$ ) and \*\* ( $P < 0.01$ ). Lp, *L. plantarum*; Lr, *L. rhamnosus*; Bb, *B. bifidum*; and Ar, arbutin.



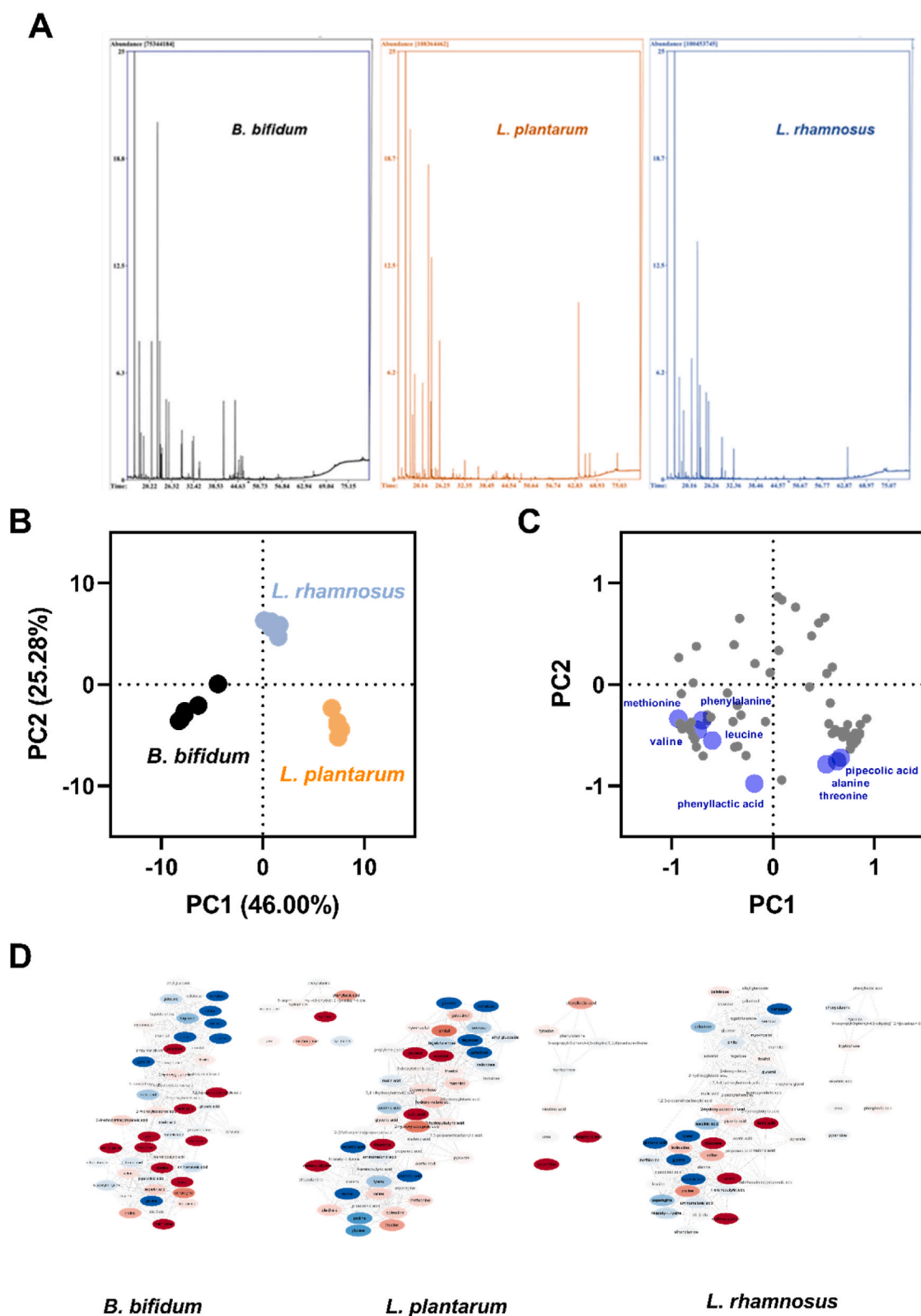


**Fig. 4.** Metabolic profiling of probiotics culture supernatants by GC-MS. (A) Representative ion chromatograms of *B. bifidum*, *L. plantarum*, and *L. rhamnosus* (negative control). (B–C) Principal component analysis identified metabolites present in bacterial culture supernatants. Score plots (B) and loading plots (C). (D) Network analysis of metabolites of *B. bifidum*, *L. plantarum*, and *L. rhamnosus* by ChemViz. Nodes represent structurally identified metabolites as indicated by different colors. Red and blue indicate increases and decreases in metabolite levels, respectively, when subtracted by the abundance of the uncultured medium components. Metabolites were clustered into amino acids, organic acids, sugars, and nucleotides. (For interpretation of the references to color in this figure legend, the reader is referred to the Web version of this article.)

Fig. 4D represent the molecular networks of metabolite abundances of each probiotic culture supernatant subtracted by its uncultured medium components. Molecular network indicating similarity in the chemical structure between the discriminatory metabolites compared to the medium components revealed that each strain produced distinct profiles of metabolites in their culture supernatants. In particular, production of amino acids and sugars increased and decreased, respectively, in *B. bifidum* than the medium, while several of the metabolites were more consumed compared to the uncultured medium components in *L. plantarum*. In *L. rhamnosus*, the abundance of only a few metabolites was changed. These results indicate that the metabolite consumption and production profile of each probiotic strain was significantly distinct.

### 3.5. Key metabolites in the selected probiotic culture supernatants

To select candidate metabolites produced by *L. plantarum* and *B. bifidum*, a Venn diagram was generated using metabolites with levels altered versus *L. rhamnosus* (Fig. 5A). The abundance of 19 and 22 metabolites increased during the growth of *B. bifidum* and *L. plantarum* compared with the abundance of *L. rhamnosus*, and we chose eight metabolites that commonly increased in the both strains: alanine, leucine, methionine, phenylalanine, threonine, valine, pipecolic acid, and phenyllactic acid.

As shown in Fig. 5B, metabolites specifically classified into nonpolar amino acids had increased abundance in both strains. When compared the metabolite production of other polar amino acids such as aspartic acid, lysine, serine and tyrosine, the abundance of these molecules in the supernatant were not significantly different or even decreased from the abundance of uncultured medium components. Interestingly, two amino acids-derived metabolites, pipecolic acid and phenyllactic acid, were identified as candidate molecules as a tyrosinase inhibitor. Pipecolic acid is an important precursor of many microbial secondary metabolites derived from lysine and significantly produced more by *L. plantarum* than *B. bifidum* (He, 2006). We also found that phenyllactic acid was

significantly produced during the growth of *B. bifidum* and *L. plantarum* and, therefore, only present in the culture supernatants but not in their uncultured media. We also found that phenyllactic acid was exclusively produced during the growth of *B. bifidum* and *L. plantarum* and that it was not produced by *L. rhamnosus*, which suggested phenyllactic acid may have been responsible for observed tyrosinase inhibitions.

In the present study, we selected eight metabolites produced by *L. plantarum* and *B. bifidum*, viz. alanine, leucine, methionine, phenylalanine, threonine, valine, pipecolic acid, and phenyllactic acid. Previously, several studies have reported these metabolites have anti-melanogenic effects. For example, alanine and leucine have been reported to have hypopigmentary effects in B16F10 melanoma cells unassociated with tyrosinase inhibition (Ishikawa et al., 2007). In Mel-Ab cell line, valine-serine dipeptide inhibited melanin synthesis by inhibiting ERK (extracellular signal regulated kinase) phosphorylation and subsequently down-regulating the protein levels of MITF and tyrosinase (H.-E. Lee et al., 2012). In neonatal human epidermal melanocyte, threonine inhibited hyperpigmentation by activating FoxO-mediated autophagy signaling and modulating melanogenesis and tyrosinase activity. Although methionine is not directly associated with tyrosinase, glutathione, a derivative of methionine, inhibited tyrosinase activity in human melanoma cells (del Marmol et al., 1993). However, with the exception of threonine, no direct association has been reported between these metabolites and tyrosinase inhibition. In addition, no previous study has examined the effect of phenylalanine, pipecolic acid, or phenyllactic acid on tyrosinase activity. Thus, the present study suggests these metabolites as novel potent tyrosinase inhibitors, which are produced by probiotics.

### 3.6. Effects of the selected metabolites on tyrosinase activity

We analyzed the tyrosinase inhibitory activities of the selected metabolites, alanine, leucine, methionine, phenylalanine, threonine, valine, pipecolic acid, and phenyllactic acid, at concentrations of 10 or

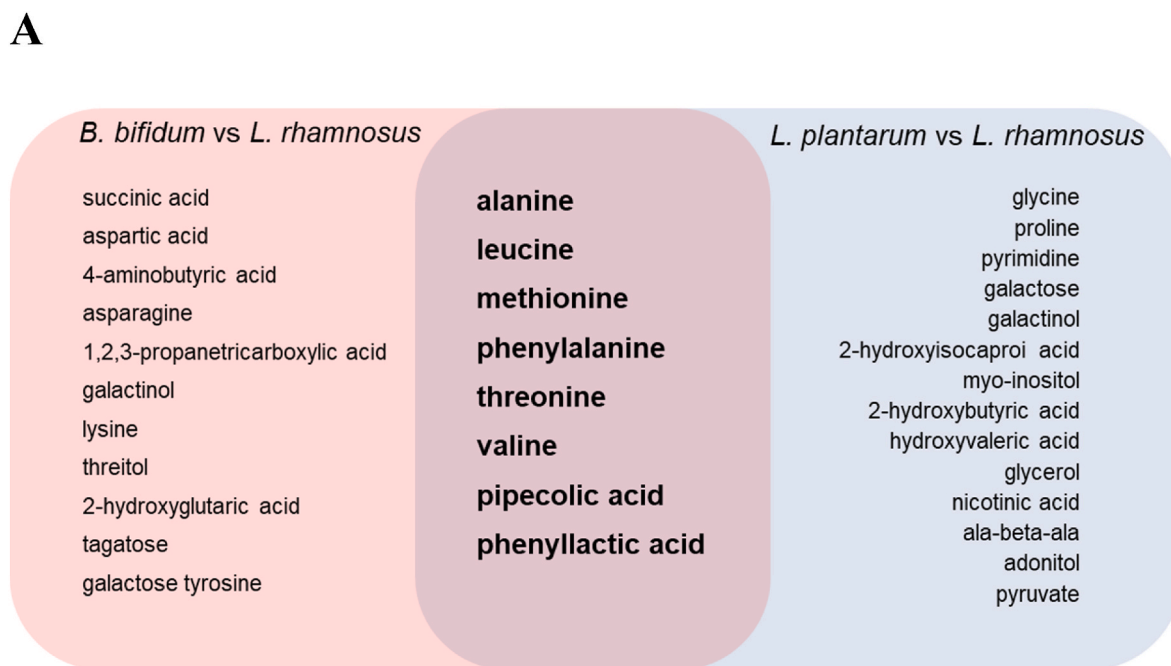


**Fig. 5.** Selected metabolites produced by *L. plantarum* and *B. bifidum*. (A) Venn diagram of metabolites significantly produced by *L. plantarum* and *B. bifidum* compared with *L. rhamnosus*. Eight metabolites that commonly increased in the both strains are indicated. (B) Abundances of eight metabolites produced by *B. bifidum*, *L. plantarum*, and *L. rhamnosus* and present in the uncultured media components. B<sub>medium</sub>, P<sub>medium</sub>, and R<sub>medium</sub> represent the uncultured media components of *B. bifidum*, *L. plantarum*, and *L. rhamnosus*, respectively. Metabolite abundances are presented in arbitrary units (AU). Data are expressed as violin plots of six determinations. The analysis was conducted by one-way ANOVA followed by Šidák test for post-hoc analysis. Significant differences are indicated as \* ( $P < 0.05$ ) and \*\* ( $P < 0.01$ ).

## B

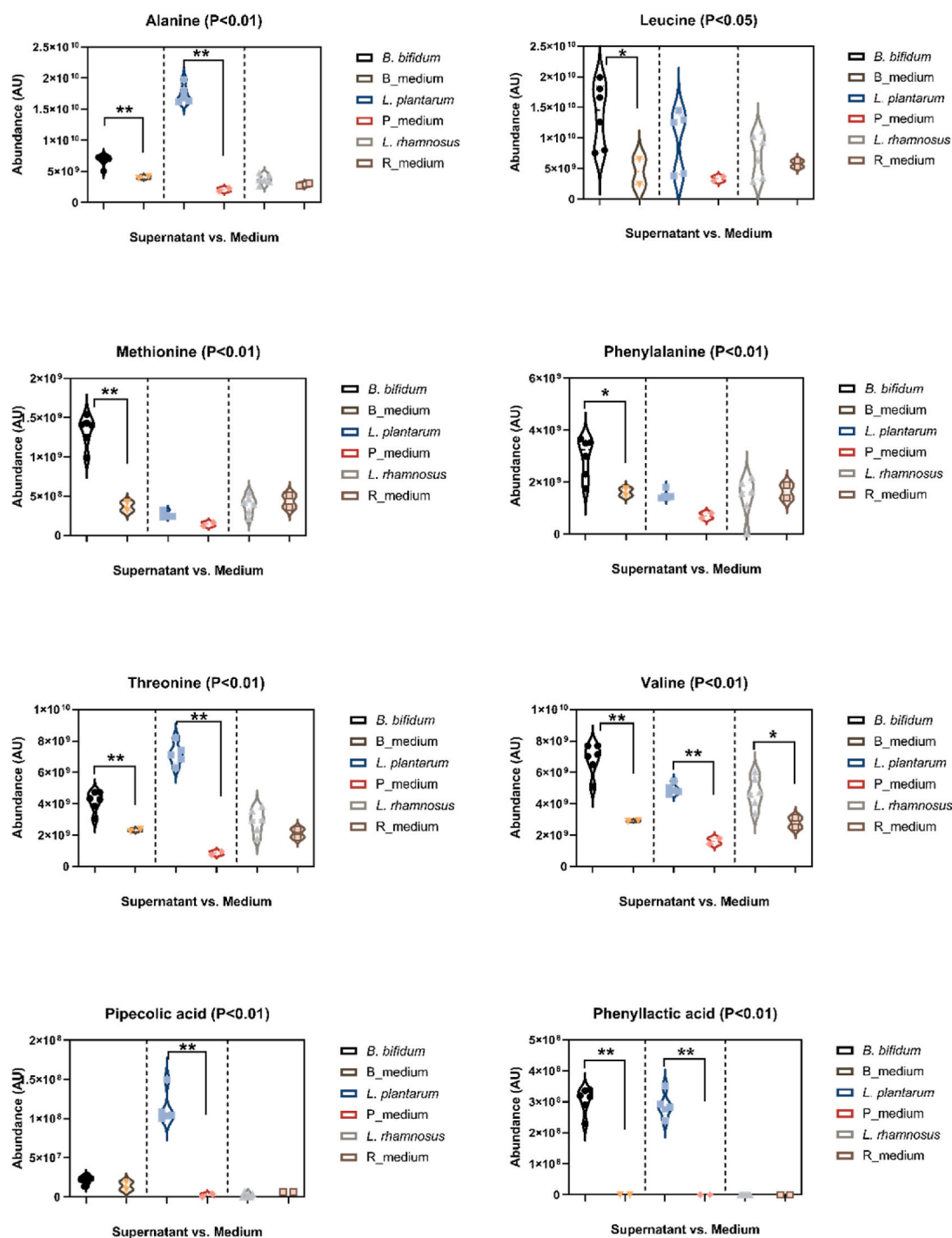
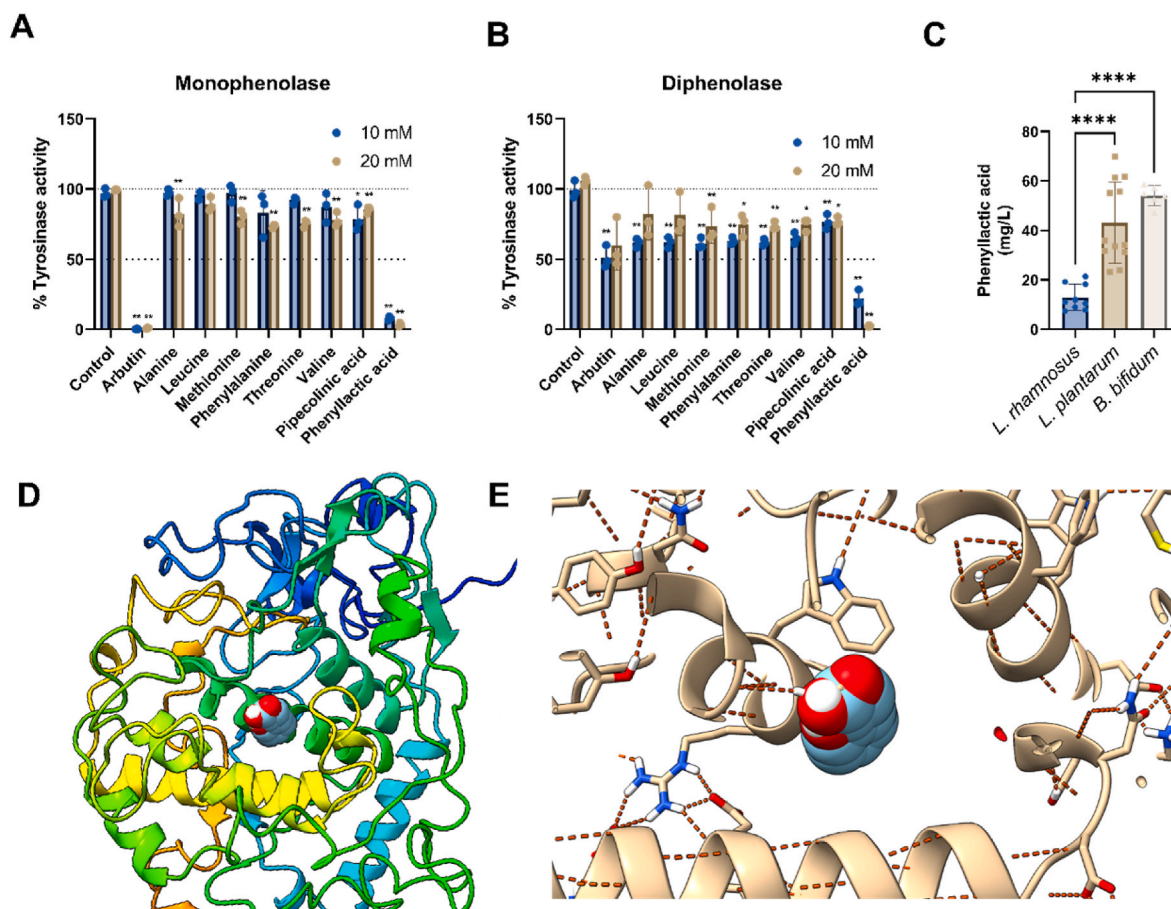


Fig. 5. (continued).

20 mM (Fig. 6A and B). Strikingly, phenyllactic acid potently and dose-dependently inhibited the tyrosinase activity. Other metabolites slightly reduced (<50%) tyrosinase activity (generally, diphenolase was more effectively inhibited than monophenolase). Further quantification of phenyllactic acid present in *L. rhamnosus*, *L. plantarum*, and *B. bifidum* confirmed higher concentration of phenyllactic acid in the culture supernatant (Fig. 6C). To investigate the interaction between phenyllactic

acid and tyrosinase, we performed an *in silico* docking simulation of the interaction between phenyllactic acid and tyrosinase (Fig. 6D). For molecular docking prediction studies, AlphaFold (ID: AF-P14679-F1-model) (Jumper et al., 2021) was used to predict the structure of human tyrosinase, which was prepared for docking using the dock prep tool in UCSF Chimera (Lang et al., 2009). Phenyllactic acid was found to bind with the active site of tyrosinase with a predicted binding energy of



**Fig. 6.** Inhibition of tyrosinase activity by the eight candidate metabolites produced by *B. bifidum* and *L. plantarum*. Monophenolase (A) and diphenolase (B) activities were assessed using L-tyrosine and L-DOPA, respectively, as substrates. Compounds were added at concentrations of 10 or 20 mM. 50% inhibition was used as the inhibitory cutoff. Data are expressed as the means  $\pm$  SDs of three independent experiments. Significant differences are indicated by \* ( $P < 0.05$ ) or \*\* ( $P < 0.01$ ) as determined by one-way ANOVA followed by post hoc Dunnett's multiple analysis versus non-treated controls. (C) Quantification of phenyllactic acid using GC-MS. Data are expressed as the means  $\pm$  SDs. Significant differences are indicated by \*\*\*\* ( $P < 0.0001$ ) as determined by one-way ANOVA followed by post hoc Tukey's multiple analysis. (D) Molecular docking of phenyllactic acid (shown as a combination of spheres) to the substrate binding site of human tyrosinase (ribbons). (E) Closed view of the predicted binding of phenyllactic acid to the catalytic site of tyrosinase showing possible hydrogen bonds.

−8.5 kcal/mol, and arbutin (the positive control) bound with a predicted value of −8.0 kcal/mol. Referring the catalytic sites of human tyrosinase that have been explored in other reports, phenyllactic acid would interact with His211 in the active site (Fig. 6E) (Noh et al., 2020). Taken together, *in silico* docking and experimental tyrosinase inhibition results indicated that phenyllactic acid is a candidate tyrosinase inhibitor with therapeutic potential.

Phenyllactic acid (2-hydroxy-3-phenylpropanoic acid) is composed of a benzene ring conjugated with propanoic acid and is a known broad-spectrum antimicrobial with antibacterial, antibiofilm, and antifungal activities (Liu et al., 2020). Recent studies have revealed its immune-modulatory effects are elicited via the HCA<sub>3</sub> (hydroxycarboxylic acid receptor 3) signaling cascade (Peters et al., 2019). Phenyllactic acid can be synthesized, but due to the limitations associated with impurities, reaction conditions, and environmental pollution, microbial production has emerged as a more attractive means (Wu et al., 2020). Interestingly, the microbial production of phenyllactic acid has been verified in lactic acid bacteria, including lactobacilli, bacilli, and clostridia, and recently in bifidobacteria (Dickert et al., 2000; Laursen et al., 2021). Chatterjee et al. reported phenyllactic acid was not cytotoxic to fish or human cell lines (Chatterjee et al., 2017). Thus, based on its safety and functionality, phenyllactic acid appears to be a promising melanogenesis inhibitor.

#### 4. Conclusions

Tyrosinase is essential for melanogenesis, and natural tyrosinase inhibitors are required to prevent food discoloration and skin pigmentation. Most of the tyrosinase inhibitors found to date were identified in plants and herbs, but recent studies have focused on the bioactive compounds with beneficial effects on human health produced by probiotics. The present study shows that culture supernatants of *L. plantarum* and *B. bifidum* inhibited melanin synthesis by targeting tyrosinase in melanin-producing cell lines. Comparative metabolomics analysis identified several metabolites produced by *L. plantarum* and *B. bifidum*, and further enzymatic studies revealed that phenyllactic acid effectively inhibited tyrosinase activity, which suggested that phenyllactic acid is a candidate tyrosinase inhibitor.

Postbiotics are beneficial bioactive compounds released by or produced during the metabolism of probiotics not containing live microorganisms. Application of postbiotics have provided safer use and higher effectiveness than administering live microorganisms known as probiotics. This study identifies the microbial metabolite phenyllactic acid as a candidate inhibitor of tyrosinase and melanogenesis. We would expect that the presence of other functional molecules produced by *L. plantarum* and *B. bifidum* in probiotic culture supernatants are likely to act synergistically and enhance the anti-melanogenic effect of phenyllactic acid.



## CRediT authorship contribution statement

**Minhye Shin:** Writing – original draft, Data curation, Methodology, Visualization. **Van-Long Truong:** Methodology, Visualization, Writing – review & editing. **Minjee Lee:** Methodology, Resources. **Donggyu Kim:** Methodology, Visualization. **Myun Soo Kim:** Methodology, Resources. **Hana Cho:** Methodology, Resources. **Young Hoon Jung:** Writing – review & editing. **Jungwoo Yang:** Conceptualization, Investigation, Resources. **Woo Sik Jeong:** Investigation, Writing – review & editing. **Younghoon Kim:** Investigation, Writing – review & editing.

## Declaration of competing interest

The authors declare the following financial interests/personal relationships which may be considered as potential competing interests: The authors have no conflict of interest to declare. The sponsors played no part in the study design, research (other than providing the probiotic strains), or manuscript preparation.

## Data availability

Data will be made available on request.

## Acknowledgements

This research was supported by the Basic Science Research Program (#2022R1C1C1008574) through the National Research Foundation of Korea.

## References

- Bourebaba, Y., Marycz, K., Mularczyk, M., Bourebaba, L., 2022. Postbiotics as potential new therapeutic agents for metabolic disorders management. *Biomedicine & Pharmacotherapy = Biomedicine & Pharmacotherapie* 153, 113138. <https://doi.org/10.1016/j.biopha.2022.113138>.
- Brenner, M., Hearing, V.J., 2008. The protective role of melanin against UV damage in human skin. *Photochem. Photobiol.* 84 (3), 539–549. <https://doi.org/10.1111/j.1751-1097.2007.00226.x>.
- Chatterjee, M., D'Morris, S., Paul, V., Warriar, S., Vasudevan, A.K., Vanuopadath, M., Nair, S.S., Paul-Prasanth, B., Mohan, C.G., Biswas, R., 2017. Mechanistic understanding of Phenyllactic acid mediated inhibition of quorum sensing and biofilm development in *Pseudomonas aeruginosa*. *Appl. Microbiol. Biotechnol.* 101 (22), 8223–8236. <https://doi.org/10.1007/s00253-017-8546-4>.
- del Marmol, V., Solano, F., Sels, A., Huez, G., Libert, A., Lejeune, F., Ghanem, G., 1993. Glutathione depletion increases tyrosinase activity in human melanoma cells. *J. Invest. Dermatol.* 101 (6), 871–874. <https://doi.org/10.1111/1523-1747.ep12371709>.
- Dickert, S., Pierik, A.J., Linder, D., Buckel, W., 2000. The involvement of coenzyme A esters in the dehydration of (R)-phenyllactate to (E)-cinnamate by *Clostridium sporogenes*. *Eur. J. Biochem.* 267 (12), 3874–3884. <https://doi.org/10.1046/j.1432-1327.2000.01427.x>.
- Ducrotte, P., Sawant, P., Jayanthi, V., 2012. Clinical trial: *Lactobacillus plantarum* 299v (DSM 9843) improves symptoms of irritable bowel syndrome. *World J. Gastroenterol.* 18 (30), 4012–4018. <https://doi.org/10.3748/wjg.v18.i30.4012>.
- Ebanks, J.P., Wickett, R.R., Boissy, R.E., 2009. Mechanisms regulating skin pigmentation: the rise and fall of complexion coloration. *Int. J. Mol. Sci.* 10 (9), 4066–4087. <https://doi.org/10.3390/ijms10094066>.
- El-Nashar, H.A.S., El-Din, M.I.G., Hritcu, L., Eldashan, O.A., 2021. Insights on the inhibitory power of flavonoids on tyrosinase activity: a survey from 2016 to 2021. *Molecules* 26 (24), 7546. <https://doi.org/10.3390/molecules26247546>.
- Fidanza, M., Panigrahi, P., Kollmann, T.R., 2021. *Lactiplantibacillus plantarum*-nomad and ideal probiotic. *Front. Microbiol.* 12, 712236. <https://doi.org/10.3389/fmicb.2021.712236>.
- He, M., 2006. Pipecolic acid in microbes: biosynthetic routes and enzymes. *J. Ind. Microbiol. Biotechnol.* 33 (6), 401–407. <https://doi.org/10.1007/s10295-006-0078-3>.
- Huang, H.-C., Huang, W.-Y., Chiu, S.-H., Ke, H.-J., Chiu, S.-W., Wu, S.-Y., Kuo, F.-S., Chang, T.-M., 2011. Antimelanogenic and antioxidative properties of *Bifidobacterium bifidum*. *Arch. Dermatol. Res.* 303 (7), 527–531. <https://doi.org/10.1007/s00403-011-1135-y>.
- Hun Son, K., Young Heo, M., 2013. Inhibitory effects of Korean indigenous plants on tyrosinase and melanogenesis. *J. Cosmet. Sci.* 64 (2), 145–158.
- Ikarashi, N., Fukuda, N., Ochiai, M., Sasaki, M., Kon, R., Sakai, H., Hatanaka, M., Kamei, J., 2020. *Lactobacillus helveticus*-fermented milk whey suppresses melanin production by inhibiting tyrosinase through decreasing MITF expression. *Nutrients* 12 (7), 2082. <https://doi.org/10.3390/nu12072082>.
- Ishihara, Y., Oka, M., Tsunakawa, M., Tomita, K., Hatori, M., Yamamoto, H., Kamei, H., Miyaki, T., Konishi, M., Oki, T., 1991. Melanostatin, a new melanin synthesis inhibitor. Production, isolation, chemical properties, structure and biological activity. *J. Antibiot.* 44 (1), 25–32. <https://doi.org/10.7164/antibiotics.44.25>.
- Ishikawa, M., Kawase, I., Ishii, F., 2007. Combination of amino acids reduces pigmentation in B16F0 melanoma cells. *Biol. Pharm. Bull.* 30 (4), 677–681. <https://doi.org/10.1248/bpb.30.677>.
- Jin, M.L., Park, S.Y., Kim, Y.H., Park, G., Son, H.-J., Lee, S.-J., 2012. Suppression of  $\alpha$ -MSH and IBMX-induced melanogenesis by cordycepin via inhibition of CREB and MITF, and activation of PI3K/Akt and ERK-dependent mechanisms. *Int. J. Mol. Med.* 29 (1), 119–124. <https://doi.org/10.3892/ijmm.2011.807>.
- Jumper, J., Evans, R., Pritzel, A., Green, T., Figurnov, M., Ronneberger, O., Tunyasuvunakool, K., Bates, R., Zidek, A., Potapenko, A., Bridgland, A., Meyer, C., Kohl, S.A.A., Ballard, A.J., Cowie, A., Romera-Paredes, B., Nikolov, S., Jain, R., Adler, J., et al., 2021. Highly accurate protein structure prediction with AlphaFold. *Nature* 596 (7873), 583–589. <https://doi.org/10.1038/s41586-021-03819-2>.
- Kim, H.R., Kim, H., Jung, B.J., You, G.E., Jang, S., Chung, D.K., 2015. Lipoteichoic acid isolated from *Lactobacillus plantarum* inhibits melanogenesis in B16F10 mouse melanoma cells. *Mol. Cell.* 38 (2), 163–170. <https://doi.org/10.14348/molcells.2015.2263>.
- Lang, P.T., Brozell, S.R., Mukherjee, S., Pettersen, E.F., Meng, E.C., Thomas, V., Rizzo, R.C., Case, D.A., James, T.L., Kuntz, I.D., 2009. DOCK 6: combining techniques to model RNA-small molecule complexes. *RNA (N. Y.)* 15 (6), 1219–1230. <https://doi.org/10.1261/rna.1563609>.
- Laursen, M.F., Sakanaka, M., von Burg, N., Mörbé, U., Andersen, D., Moll, J.M., Pekmez, C.T., Rivollier, A., Michaelsen, K.F., Mølgaard, C., Lind, M.V., Dragsted, L.O., Katayama, T., Frandsen, H.L., Vinggaard, A.M., Bahl, M.I., Brix, S., Agace, W., Licht, T.R., Roager, H.M., 2021. *Bifidobacterium* species associated with breastfeeding produce aromatic lactic acids in the infant gut. *Nature Microbiol.* 6 (11) <https://doi.org/10.1038/s41564-021-00970-4>. Article 11.
- Lee, H.-E., Kim, E.-H., Choi, H.-R., Sohn, U.D., Yun, H.-Y., Baek, K.J., Kwon, N.S., Park, K.-C., Kim, D.-S., 2012. Dipeptides inhibit melanin synthesis in mel-ab cells through down-regulation of tyrosinase. *Korean J. Physiol. Pharmacol.: Off. J. Korean Physiol. Soc. Korean Soc. Pharmacol.* 16 (4), 287–291. <https://doi.org/10.4196/kjpp.2012.16.4.287>.
- Lee, S., Park, H.-O., Yoo, W., 2022. Anti-melanogenic and antioxidant effects of cell-free supernatant from *Lactobacillus gasseri* BN17. *Microorganisms* 10 (4), 788. <https://doi.org/10.3390/microorganisms10040788>.
- Lim, H.Y., Jeong, D., Park, S.H., Shin, K.K., Hong, Y.H., Kim, E., Yu, Y.-G., Kim, T.-R., Kim, H., Lee, J., Cho, J.Y., 2020. Antiwrinkle and antimelanogenesis effects of tyndallized *Lactobacillus acidophilus* KCCM12625P. *Int. J. Mol. Sci.* 21 (5) <https://doi.org/10.3390/ijms21051620>.
- Liu, F., Sun, Z., Wang, F., Liu, Y., Zhu, Y., Du, L., Wang, D., Xu, W., 2020. Inhibition of biofilm formation and exopolysaccharide synthesis of *Enterococcus faecalis* by phenyllactic acid. *Food Microbiol.* 86, 103344. <https://doi.org/10.1016/j.fm.2019.103344>.
- Mason, H.S., 1948. The chemistry of melanin; mechanism of the oxidation of dihydroxyphenylalanine by tyrosinase. *J. Biol. Chem.* 172 (1), 83–99.
- Metsalu, T., Vilo, J., 2015. ClustVis: a web tool for visualizing clustering of multivariate data using Principal Component Analysis and heatmap. *Nucleic Acids Res.* 43 (W1), W566–W570. <https://doi.org/10.1093/nar/gkv468>.
- Muñoz-Muñoz, J.L., Acosta-Motos, J.R., García-Molina, F., Varon, R., García-Ruiz, P.A., Tudela, J., García-Cánovas, F., Rodríguez-López, J.N., 2010. Tyrosinase inactivation in its action on dopa. *Biochim. Biophys. Acta, Proteins Proteomics* 1804 (7), 1467–1475. <https://doi.org/10.1016/j.bbapap.2010.02.015>.
- Nataraj, B.H., Ali, S.A., Behare, P.V., Yadav, H., 2020. Postbiotics-parabiotics: the new horizons in microbial biotechnology and functional foods. *Microb. Cell Factories* 19 (1), 168. <https://doi.org/10.1186/s12934-020-01426-w>.
- Noh, H., Lee, S.-J., Jo, H.-J., Choi, H.W., Hong, S., Kong, K.-H., 2020. Histidine residues at the copper-binding site in human tyrosinase are essential for its catalytic activities. *J. Enzym. Inhib. Med. Chem.* 35 (1), 726–732. <https://doi.org/10.1080/14756366.2020.1740691>.
- Park, M.R., Ryu, S., Maburutse, B.E., Oh, N.S., Kim, S.H., Oh, S., Jeong, S.-Y., Jeong, D.-Y., Oh, S., Kim, Y., 2018. Probiotic *Lactobacillus fermentum* strain JDFM216 stimulates the longevity and immune response of *Caenorhabditis elegans* through a nuclear hormone receptor. *Sci. Rep.* 8 (1), 7441. <https://doi.org/10.1038/s41598-018-25333-8>.
- Pavan, W.J., Sturm, R.A., 2019. The genetics of human skin and hair pigmentation. *Annu. Rev. Genom. Hum. Genet.* 20, 41–72. <https://doi.org/10.1146/annurev-genom-083118-015230>.
- Peters, A., Krumholz, P., Jäger, E., Heintz-Buschart, A., Çakir, M.V., Rothmund, S., Gaudi, A., Ceglarek, U., Schöneberg, T., Stäubert, C., 2019. Metabolites of lactic acid bacteria present in fermented foods are highly potent agonists of human hydroxycarboxylic acid receptor 3. *PLoS Genet.* 15 (5), e1008145. <https://doi.org/10.1371/journal.pgen.1008145>.
- Raper, H.S., 1928. The aerobic oxidases. *Physiol. Rev.* 8 (2), 245–282. <https://doi.org/10.1152/physrev.1928.8.2.245>.
- Rodríguez-Pastén, A., Pérez-Hernández, N., Añorve-Morga, J., Jiménez-Alvarado, R., Carriño-Cortés, R., Sosa-Lozada, T., Fernández-Martínez, E., 2022. The activity of prebiotics and probiotics in hepatogastrointestinal disorders and diseases associated with metabolic syndrome. *Int. J. Mol. Sci.* 23 (13), 7229. <https://doi.org/10.3390/ijms23137229>.
- Shin, M., Ban, O.-H., Jung, Y.H., Yang, J., Kim, Y., 2021. Genomic characterization and probiotic potential of *Lactobacillus casei* IDCC 3451 isolated from infant faeces. *Lett. Appl. Microbiol.* 72 (5), 578–588. <https://doi.org/10.1111/lam.13449>.

- Slominski, A., Moellmann, G., Kuklinska, E., 1989. L-tyrosine, L-dopa, and tyrosinase as positive regulators of the subcellular apparatus of melanogenesis in Bomirski Ab amelanotic melanoma cells. *Pigm. Cell Res.* 2 (2), 109–116. <https://doi.org/10.1111/j.1600-0749.1989.tb00170.x>.
- Souza, P.M., Elias, S.T., Simeoni, L.A., de Paula, J.E., Gomes, S.M., Guerra, E.N.S., Fonseca, Y.M., Silva, E.C., Silveira, D., Magalhães, P.O., 2012. Plants from Brazilian Cerrado with potent tyrosinase inhibitory activity. *PLoS One* 7 (11), e48589. <https://doi.org/10.1371/journal.pone.0048589>.
- Trott, O., Olson, A.J., 2010. AutoDock Vina: improving the speed and accuracy of docking with a new scoring function, efficient optimization, and multithreading. *J. Comput. Chem.* 31 (2), 455–461. <https://doi.org/10.1002/jcc.21334>.
- Tsai, W.-H., Chou, C.-H., Chiang, Y.-J., Lin, C.-G., Lee, C.-H., 2021. Regulatory effects of *Lactobacillus plantarum*-GMNL6 on human skin health by improving skin microbiome. *Int. J. Med. Sci.* 18 (5), 1114–1120. <https://doi.org/10.7150/ijms.51545>.
- Turroni, F., Duranti, S., Bottacini, F., Guglielmetti, S., Van Sinderen, D., Ventura, M., 2014. *Bifidobacterium bifidum* as an example of a specialized human gut commensal. *Front. Microbiol.* 5, 437. <https://doi.org/10.3389/fmicb.2014.00437>.
- Turroni, F., Peano, C., Pass, D.A., Foroni, E., Severgnini, M., Claesson, M.J., Kerr, C., Hourihane, J., Murray, D., Fuligni, F., Gueimonde, M., Margolles, A., De Bellis, G., O'Toole, P.W., van Sinderen, D., Marchesi, J.R., Ventura, M., 2012. Diversity of bifidobacteria within the infant gut microbiota. *PLoS One* 7 (5), e36957. <https://doi.org/10.1371/journal.pone.0036957>.
- Wang, J., Ji, H., Wang, S., Liu, H., Zhang, W., Zhang, D., Wang, Y., 2018. Probiotic *Lactobacillus plantarum* promotes intestinal barrier function by strengthening the epithelium and modulating gut microbiota. *Front. Microbiol.* 9, 1953. <https://doi.org/10.3389/fmicb.2018.01953>.
- Wu, W., Deng, G., Liu, C., Gong, X., Ma, G., Yuan, Q., Yang, E., Li, X., Luo, Y., 2020. Optimization and multiomic basis of phenyllactic acid overproduction by *Lactobacillus plantarum*. *J. Agric. Food Chem.* 68 (6), 1741–1749. <https://doi.org/10.1021/acs.jafc.9b07136>.
- Yu, Y., Dunaway, S., Champer, J., Kim, J., Alikhan, A., 2020. Changing our microbiome: probiotics in dermatology. *Br. J. Dermatol.* 182 (1), 39–46. <https://doi.org/10.1111/bjd.18088>.
- Zhou, Q., Xue, B., Gu, R., Li, P., Gu, Q., 2021. *Lactobacillus plantarum* ZJ316 attenuates *Helicobacter pylori*-induced gastritis in C57BL/6 mice. *J. Agric. Food Chem.* 69 (23), 6510–6523. <https://doi.org/10.1021/acs.jafc.1c01070>.
- Zolghadri, S., Bahrani, A., Hassan Khan, M.T., Munoz-Munoz, J., Garcia-Molina, F., Garcia-Canovas, F., Saboury, A.A., 2019. A comprehensive review on tyrosinase inhibitors. *J. Enzym. Inhib. Med. Chem.* 34 (1), 279–309. <https://doi.org/10.1080/14756366.2018.1545767>.